

Supporting Information

Surface modification of polymer nanoparticles with native albumin for enhancing drug delivery to solid tumors

Hyesun Hyun, Joonyoung Park, Kiela Willis, Ji Eun Park, L. Tiffany Lyle, Woojin Lee, Yoon Yeo

4 Supporting Tables

16 Supporting Figures

Table S1. Size and zeta potential of NPs^a

NP type	z-average (d.nm)	Polydispersity index (PI)	Zeta potential (mV)
NP	181 ± 18	0.08 ± 0.04	-2.4 ± 0.7
NP-pD	188 ± 28	0.09 ± 0.08	-3 ± 1
NP/Al	174 ± 13	0.08 ± 0.06	-3 ± 1
NPxAl	173 ± 36	0.12 ± 0.06	-15 ± 4
NP-pD-Al	185 ± 11	0.06 ± 0.02	-6 ± 3

^a PLGA NPs made of unlabeled PLGA.

n = 5 identically and independently prepared samples (mean ± standard deviation)

Table S2. Size of rhodamine-labeled NPs in 50% FBS

NP type	z-average (d.nm)	Polydispersity index (PI)
NP	105	0.54
NP-pD	116	0.42
NP/Al	113	0.47
NPxAl	100	0.32
NP-pD-Al	107	0.38
NP-pD-PEG	111	0.54

NPs were suspended in 50% FBS to 0.1 mg/mL. The size and PI the NPs were measured by a Malvern Zetasizer Nano ZS90.

Table S3. Size, zeta potential and loading efficiency of PTX loaded NPs^a

name	z-average (d.nm)	Polydispersity index (PI)	Zeta potential (mV)	PTX loading efficiency (LE %)
PTX@NPxAl	169 ± 5	0.12 ± 0.02	-13 ± 1	7.9 ± 1.1
PTX@NP-pD-Al	183 ± 4	0.10 ± 0.02	-3.6 ± 0.3	3.4 ± 0.3

^a PLGA NPs made of unlabeled PLGA.

n = 6 identically and independently prepared samples (mean ± s.d.)

Table S4. Serum chemistry of B16F10 tumor bearing mice at 24 h after the last treatment of PBS, PTX@NPxAl, or PTX@NP-pD-Al

Groups	Parameters (Ref. Range)				
	GLU (90-192 mg/dL)	CREA (0.20-0.80 mg/dL)	ALT (28-132 IU/L)	ALKP (62-209 IU/L)	GGT (IU/L)
PBS	185	0.2	450	69	54
	202	0.1	44	113	19
PTX@NPxAl	255	0.3	>2000	68	37
	178	0.2	898	76	17
	265	0.3	2923	98	37
	211	0.2	781	88	16
	166	0.1	1069	107	47
PTX@NP- pD-Al	224	0.2	1147	84	29
	181	0.1	62	72	16
	158	0.1	88	85	73
	170	0.2	70	86	28

Mice were treated with PBS (n = 2), PTX@NPxAl (n = 5), or PTX@NP-pD-Al (n = 4) at 15 mg/kg q3d × 2. One day after the second dose, mice were sacrificed for the analysis of serum chemistry. GLU, glucose; CREA, creatinine; ALT, alanine aminotransferase; ALKP, alkaline phosphatase; GGT, gamma glutamyl transferase.

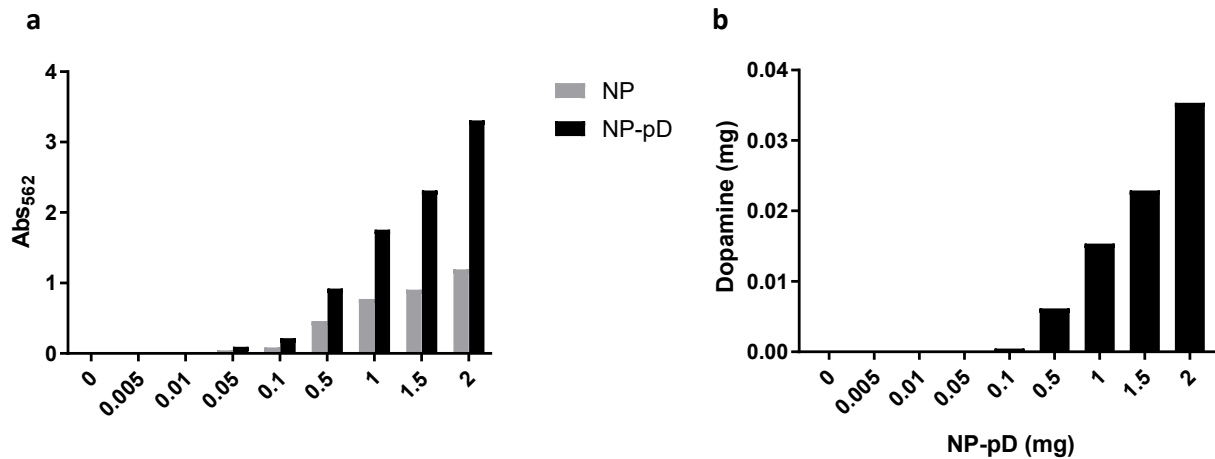


Fig. S1. Micro BCA assay of NP and NP-pD. (a) Absorbance (562 nm) difference between NP and NP-pD at different concentrations indicating the presence of pD. (b) The pD content in the NP-pD, estimated based on the absorbance difference between NP-pD and bare NP. Dopamine, NP, or NP-pD at different concentrations was incubated in the BCA working reagent for 2 h at 37 °C. A supernatant was separated from the NP suspension by centrifugation, and its absorbance was read at 562 nm. The pD content in NP-pD was estimated based on the absorbance difference between NP-pD and bare NP and a calibration curve drawn with dopamine solutions of known concentrations.

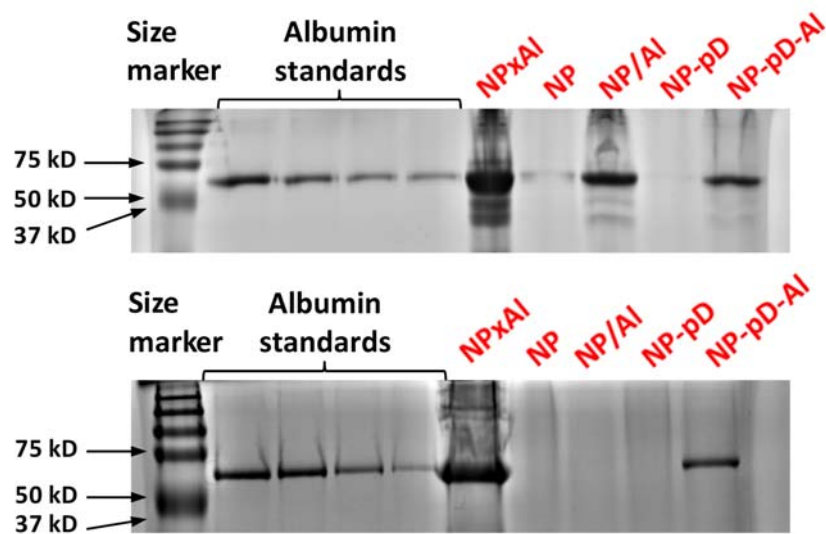


Fig. S2. Two representative SDS-PAGE gels for determination of albumin contents in NPs. Albumin standards were prepared as (Top) 0.0625, 0.03125, 0.015625 and 0.0125 mg/mL and (Bottom) 0.1, 0.08, 0.04 and 0.02 mg/mL.

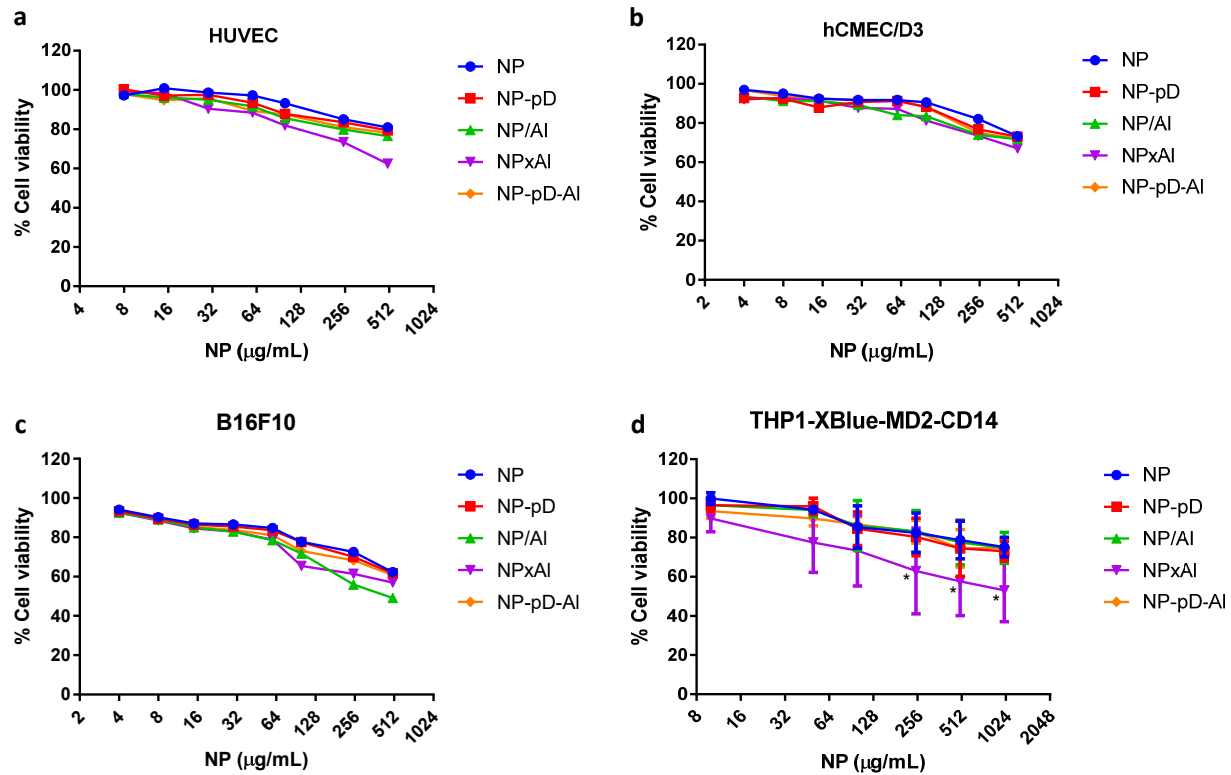


Fig. S3. Cell viability of (a) HUVEC and (b) hCMEC/D3 cells incubated with NPs (0-0.5 mg/mL) for 6 h; (c) B16F10 melanoma cells incubated with NPs (0-0.5 mg/mL) for 24 h; and (d) THP1-XBlue-MD2-CD14 cells incubated with NPs (0-1 mg/mL) for 24 h, in media supplemented with 2% (HUVEC and hCMEC/D3 cells) or 10% (B16F10 and THP1-XBlue-MD2-CD14 cells) FBS, determined by MTT assay ($n = 3-4$ identically and independently prepared samples. mean \pm s.d.). *: $p < 0.05$ vs. NP by Dunnett's multiple comparisons test following two-way ANOVA.

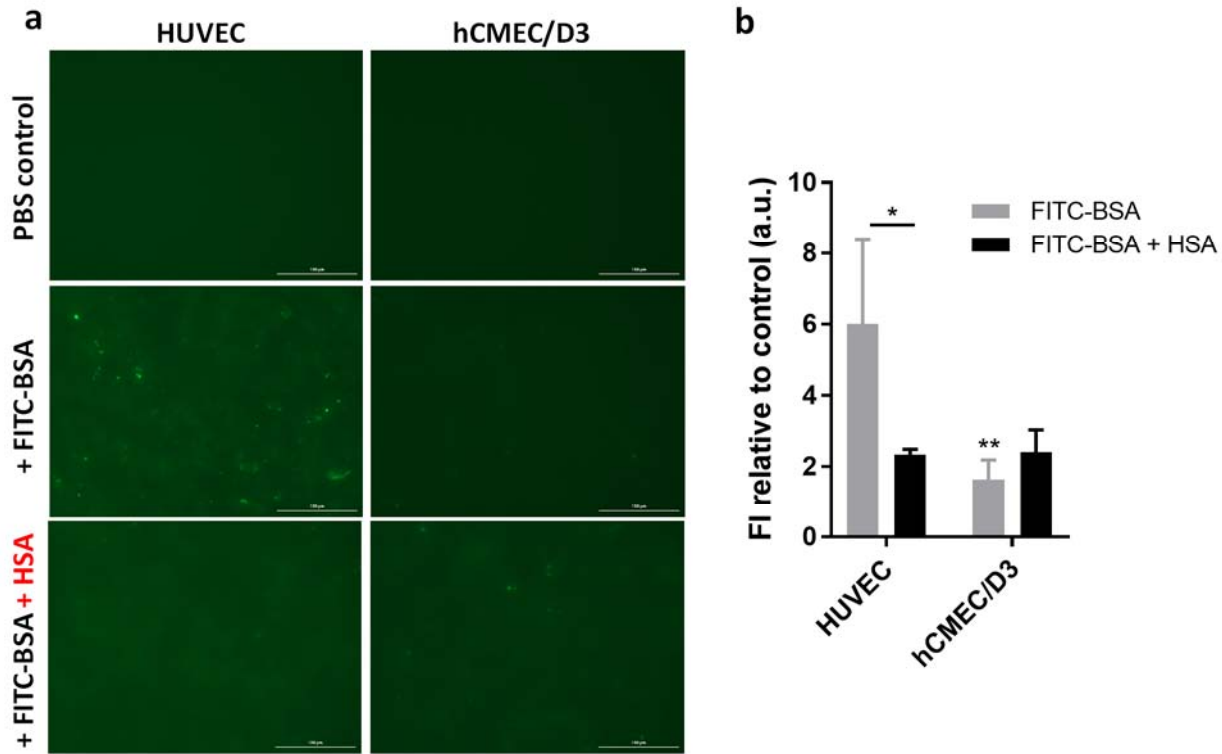


Fig. S4. Cells were incubated with PBS (control), FITC-BSA (0.8 mg/mL) alone or co-incubated with FITC-BSA and HSA (1.6 mg/mL) in the 10% serum-supplemented medium for 30 min. (a) Cells were imaged without fixation by a Biotek Cytation 3 cell imaging multimode reader. Scale bars = 100 μ m. (b) FITC-BSA interactions with HUVEC or hCMEC/D3 were determined by flow cytometry. $n = 3$ identically and independently prepared samples (mean \pm s.d.) *: $p < 0.05$; **: $p < 0.01$ vs. HUVEC with a corresponding treatment, by Sidak's multiple comparisons test following two-way ANOVA.

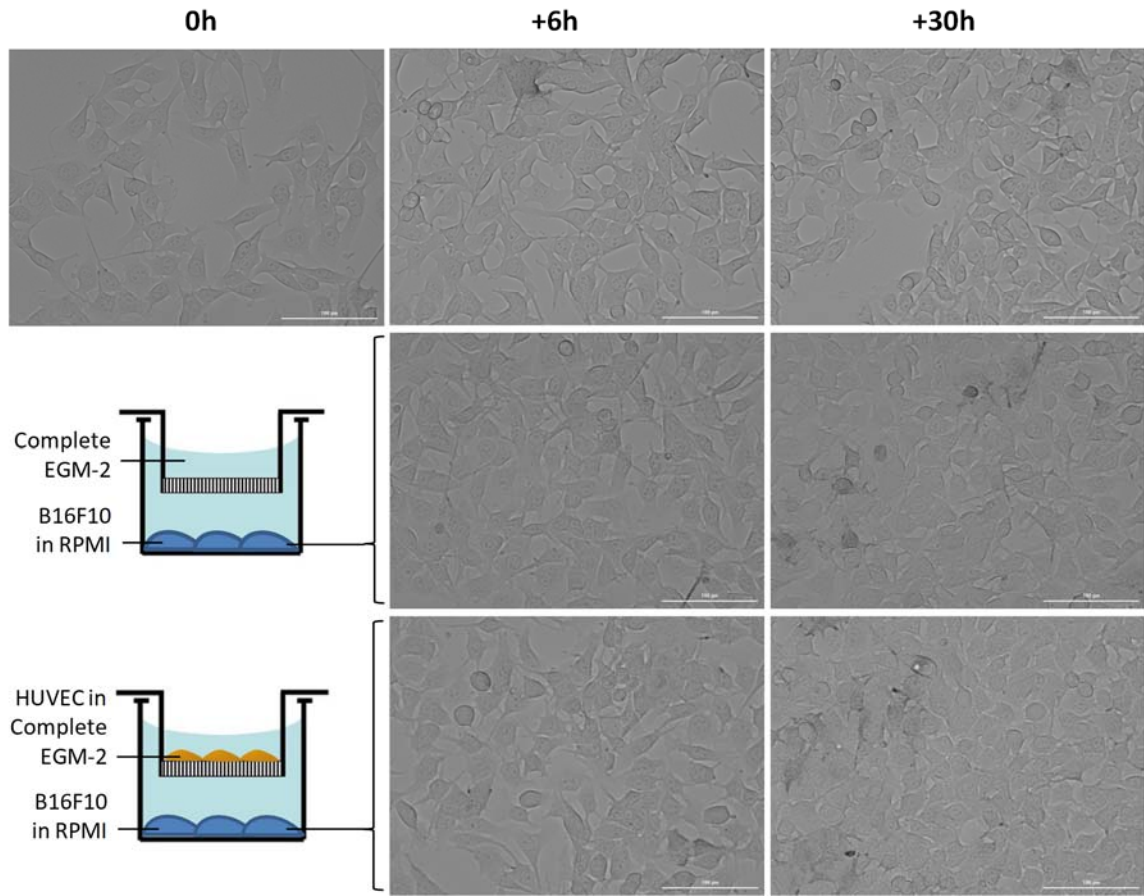


Fig. S5. Images of B16F10 cells after 6 and 30 h (6+24 h) incubation with complete EGM-2 media \pm HUVEC seeded on the Transwell insert. Scale bar: 100 μ m.

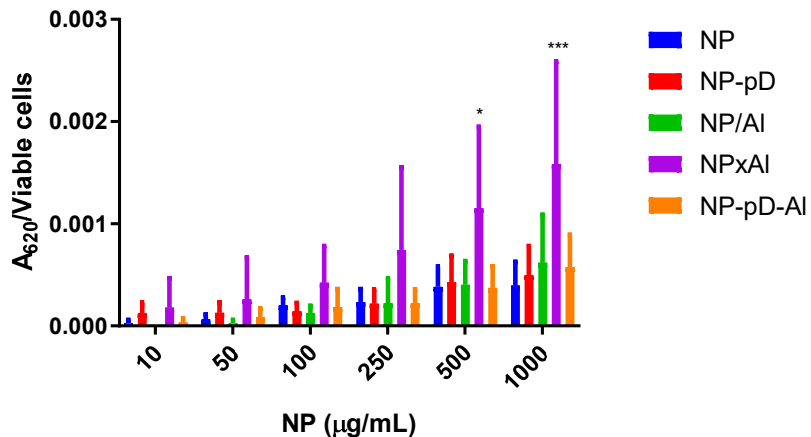


Fig. S6. SEAP levels normalized to cell viability. THP1-XBlue-MD2-CD14 cells incubated with NPs (0.1 mg/mL) for 24 h, and the supernatants were analyzed for the production of SEAP. $n = 3$ identically and independently prepared samples (mean \pm s.d.). *: $p < 0.05$; ***: $p < 0.001$ vs. NP by Dunnett's multiple comparisons test following two-way ANOVA.

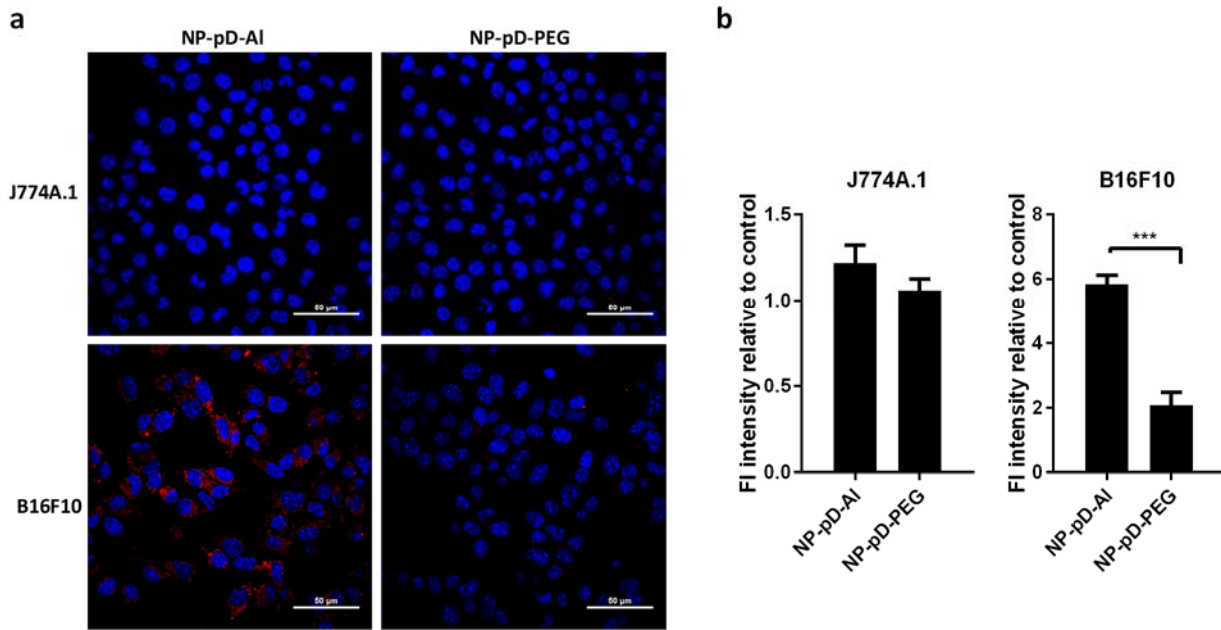


Fig. S7. Cellular uptake of NP-pD-Al and NP-pD-PEG (0.1 mg/mL) by J774A.1 macrophages after 30 min incubation and B16F10 cells after 1 h incubation in media supplemented with 10% serum. (a) Imaged by confocal microscopy (Red: rhodamine-labeled NPs; Blue: nuclei stained with Hoechst 33342). Scale bar: 50 μ m. (b) Quantified by flow cytometry. n = 3 repeated tests of the same batch NPs. NP-pD-PEG was produced by incubating NP-pD with methoxyl polyethylene glycol 2000 Da (mPEG; Nanocs, New York, NY) at an mPEG-to-NP weight ratio of 2/1 for 30 min in Tris buffer (10 mM, pH 8.5). The NP-pD-PEG was collected by centrifugation at 13,600 rcf for 20 min at 4 °C and washed twice with DI water.

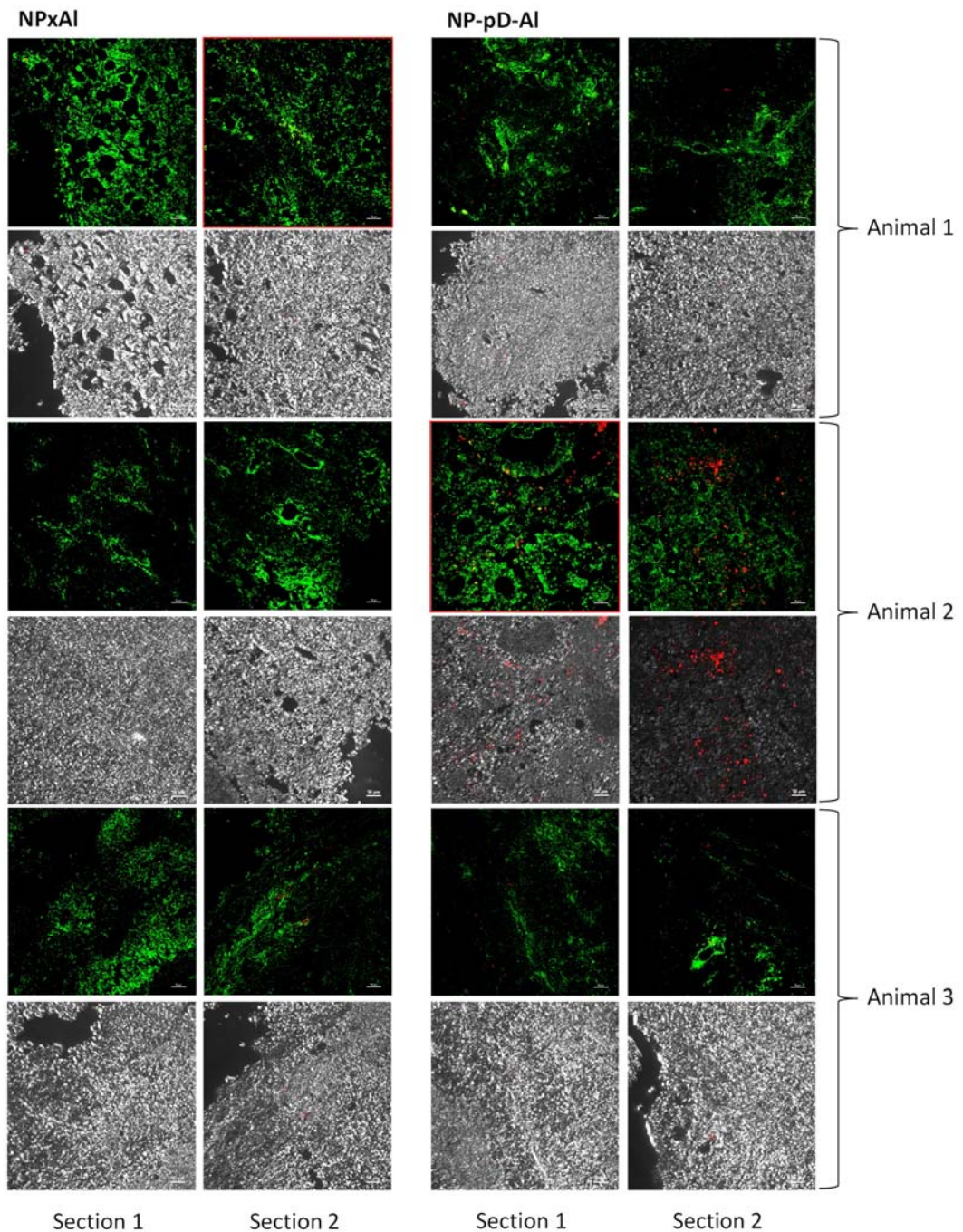


Fig. S8. All images of fluorescently labeled NPs (red) in FITC-lectin stained **tumor** blood vessels (green). A series of z-stack images were collected from two randomly selected fields per slide (16- μm cryostat section) at 0.5 μm intervals and presented as projection images. Mice ($n=3$ per group) were given a single IV injection of fluorescently labeled NPxAl or NP-pD-Al at 300 mg NP/kg. After 24 h, mice were injected IV with lectin-FITC (100 μL , 1 mg/mL in saline), perfused with saline 5 min later and sacrificed. Scale bars = 50 μm . Images used in the main text are highlighted with red outline.

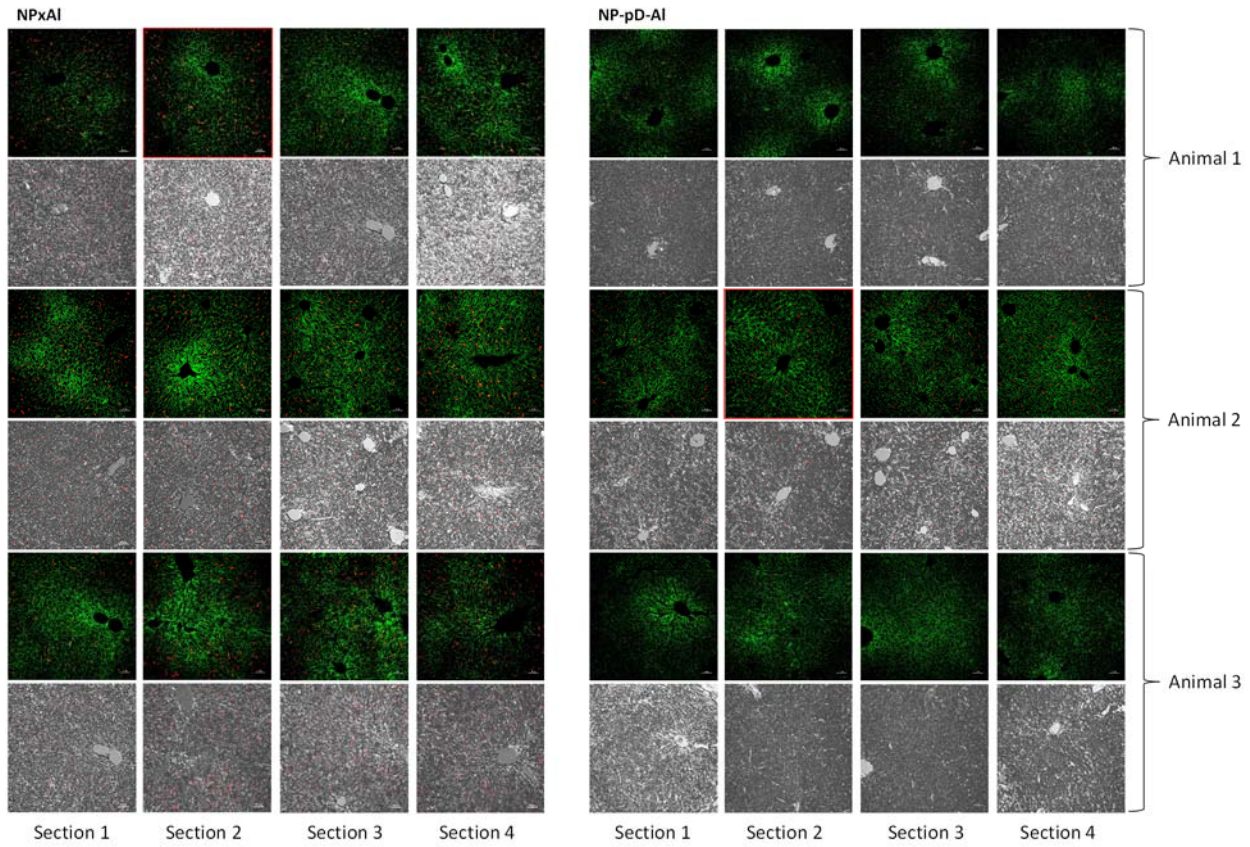


Fig. S9. All images of fluorescently labeled NPs (red) in FITC-lectin stained liver blood vessels (green). A series of z-stack images were collected from four randomly selected fields per slide (16- μ m cryostat section) at 0.5 μ m intervals and presented as projection images. Mice (n=3 per group) were given a single IV injection of fluorescently labeled NPxAl or NP-pD-Al at 300 mg NP/kg. After 24 h, mice were injected IV with lectin-FITC (100 μ L, 1 mg/mL in saline), perfused with saline 5 min later and sacrificed. Scale bars = 50 μ m. Images used in the main text are highlighted with red outline.

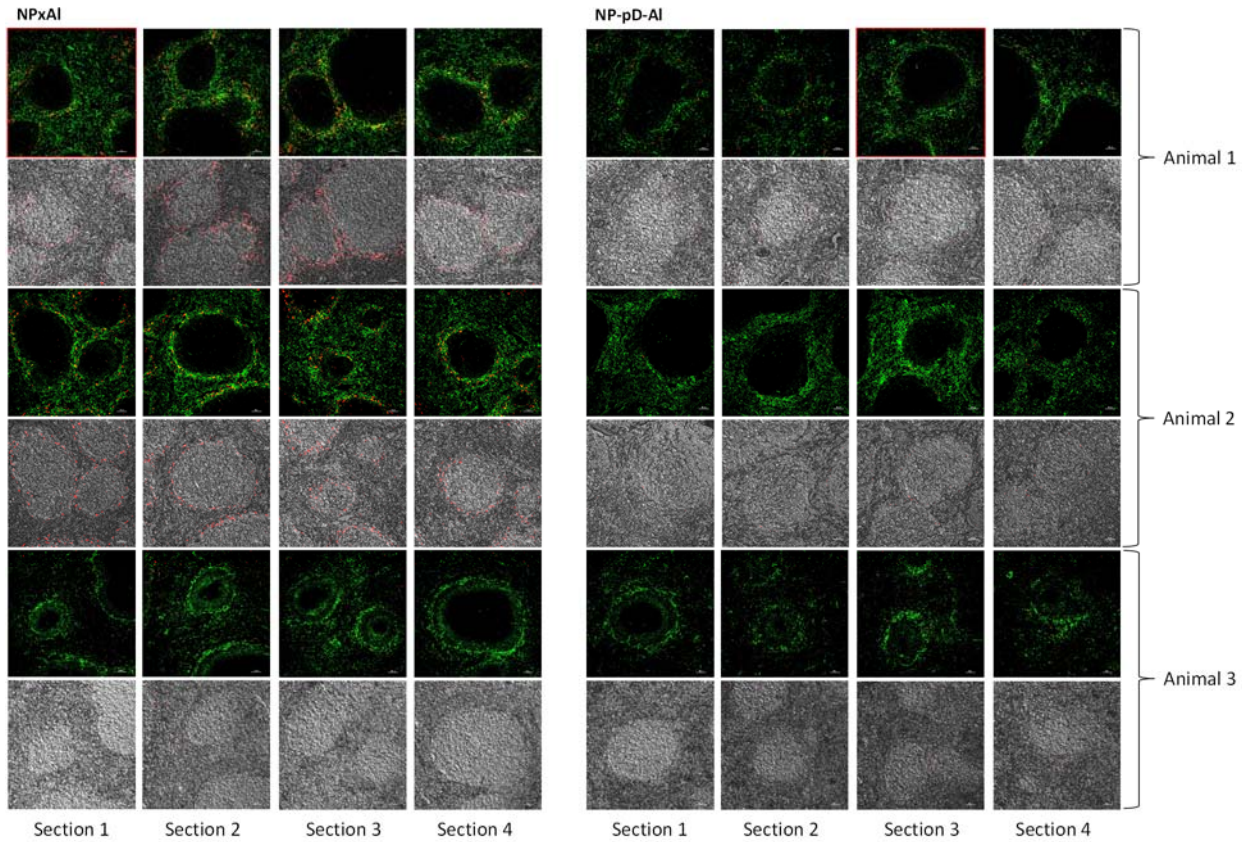


Fig. S10. All images of fluorescently labeled NPs (red) in FITC-lectin stained **spleen** blood vessels (green). A series of z-stack images were collected from four randomly selected fields per slide (16- μ m cryostat section) at 0.5 μ m intervals and presented as projection images. Mice (n=3 per group) were given a single IV injection of fluorescently labeled NPxAl or NP-pD-Al at 300 mg NP/kg. After 24 h, mice were injected IV with lectin-FITC (100 μ L, 1 mg/mL in saline), perfused with saline 5 min later and sacrificed. Scale bars = 50 μ m. Images used in the main text are highlighted with red outline.

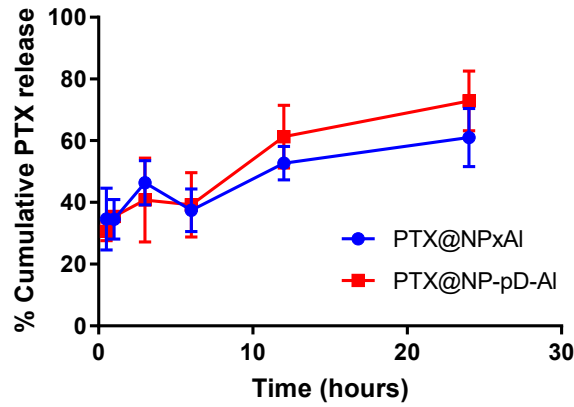


Fig. S11. Release kinetics of PTX/NPs in PBST (PBS containing 0.2% Tween 80).

PTX@NPxAl or PTX@NP-pD-Al were suspended in PBS containing 0.2% Tween 80 (PBST) to a concentration equivalent to PTX 4 μ g/mL. The NP suspensions were divided into multiple 1 mL aliquots and incubated at 37 °C with constant agitation. At each time point, the aliquots were centrifuged to separate NP pellets and supernatants. The supernatant was analyzed using HPLC. n=3 tests with representative batches (mean \pm s.d.).

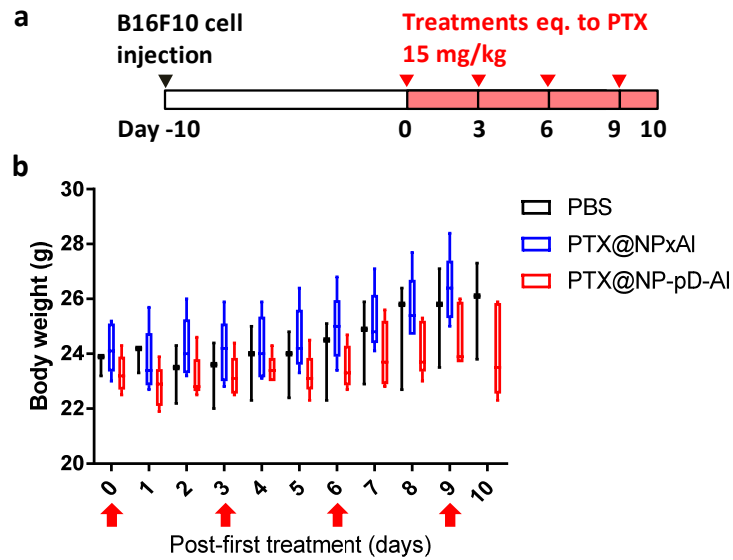


Fig. S12. (a) Dosing schedule of PTX-loaded NPs and (b) body weight change of animals. PBS (black; n = 3); PTX@NPxAl (blue; n = 5); PTX@NP-pD-Al (red; n = 5). Arrows indicate treatment times.

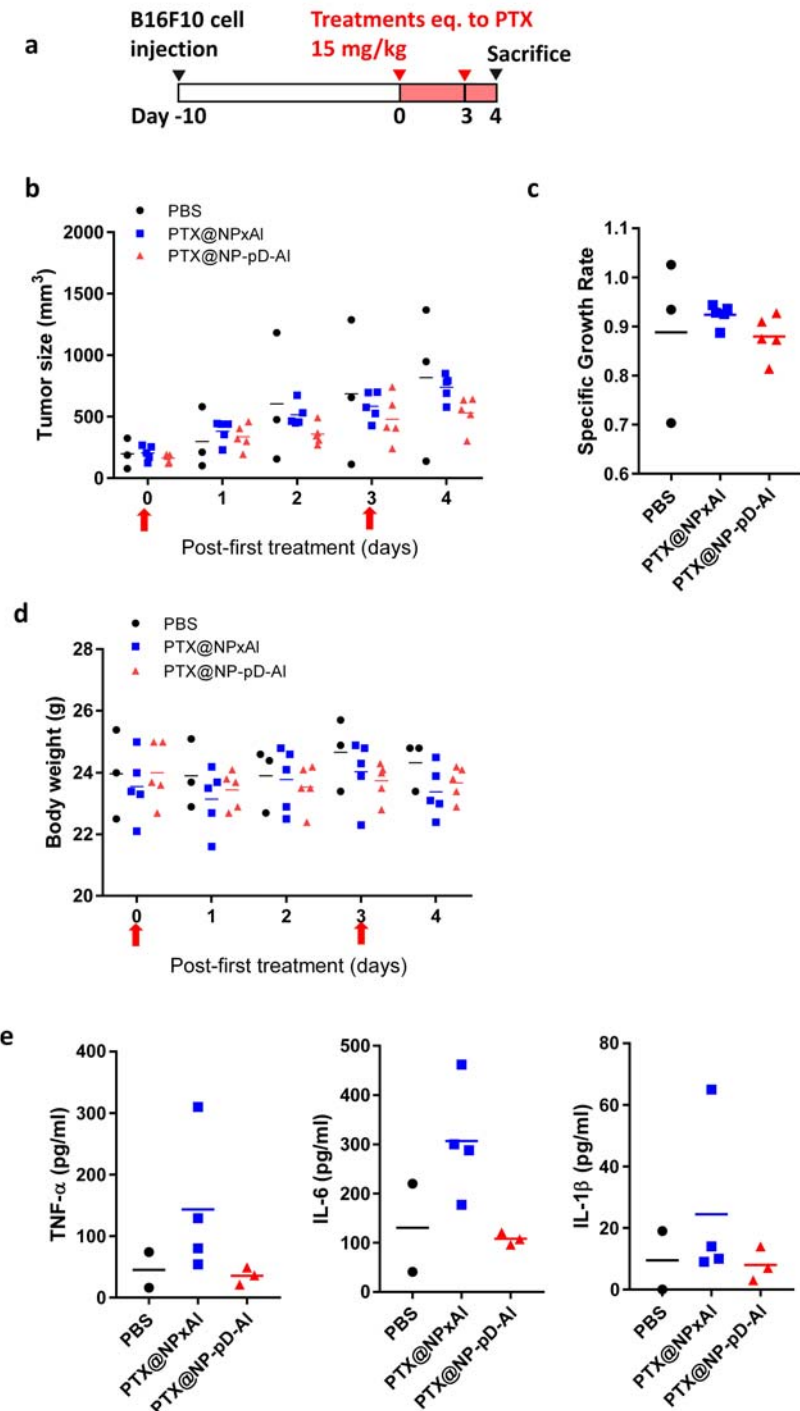


Fig. S13. In vivo activity of PTX@NPxAl and @NP-pD-Al in C57BL/6 mice. Mice were treated with PBS ($n = 3$), PTX@NPxAl ($n = 5$), or PTX@NP-pD-Al ($n = 5$) at 15 mg/kg q3d \times 2. Arrows indicate treatment times. (a) Dosing schedule of PTX-loaded NPs, (b) tumor size (mm^3), (c) specific growth rate of B16F10 tumor = $\Delta \log V / \Delta t$ (V : tumor volumes; t : time in days), (d) body weight change of animals, and (e) serum levels of TNF- α , IL-6, and IL-1 β in B16F10-tumor bearing mice treated with PBS ($n = 2$), PTX@NPxAl ($n = 4$) or PTX@NP-pD-Al ($n = 3$).

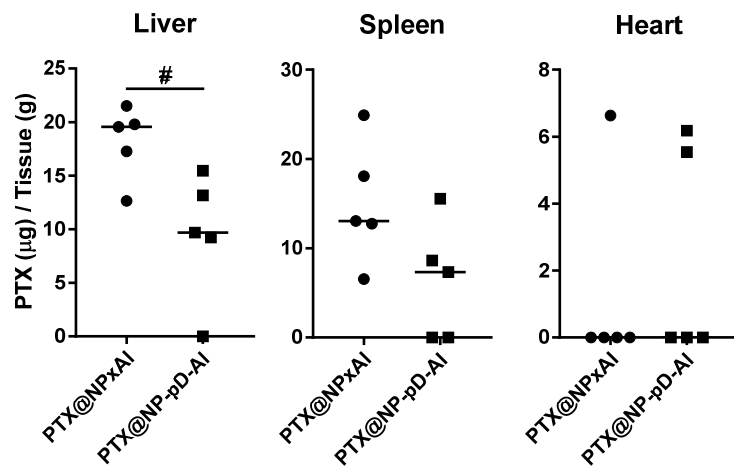


Fig. S14. PTX content in liver, spleen, and heart of B16F10 tumor-bearing mice. Mice were treated with PBS (n = 3), PTX@NPxAl (n = 5), or PTX@NP-pD-Al (n = 5) at a dose equivalent to PTX 15 mg/kg q3d × 2. One day after the second dose, mice were sacrificed for the analysis. #: p < 0.05 by non-parametric Mann-Whitney test.

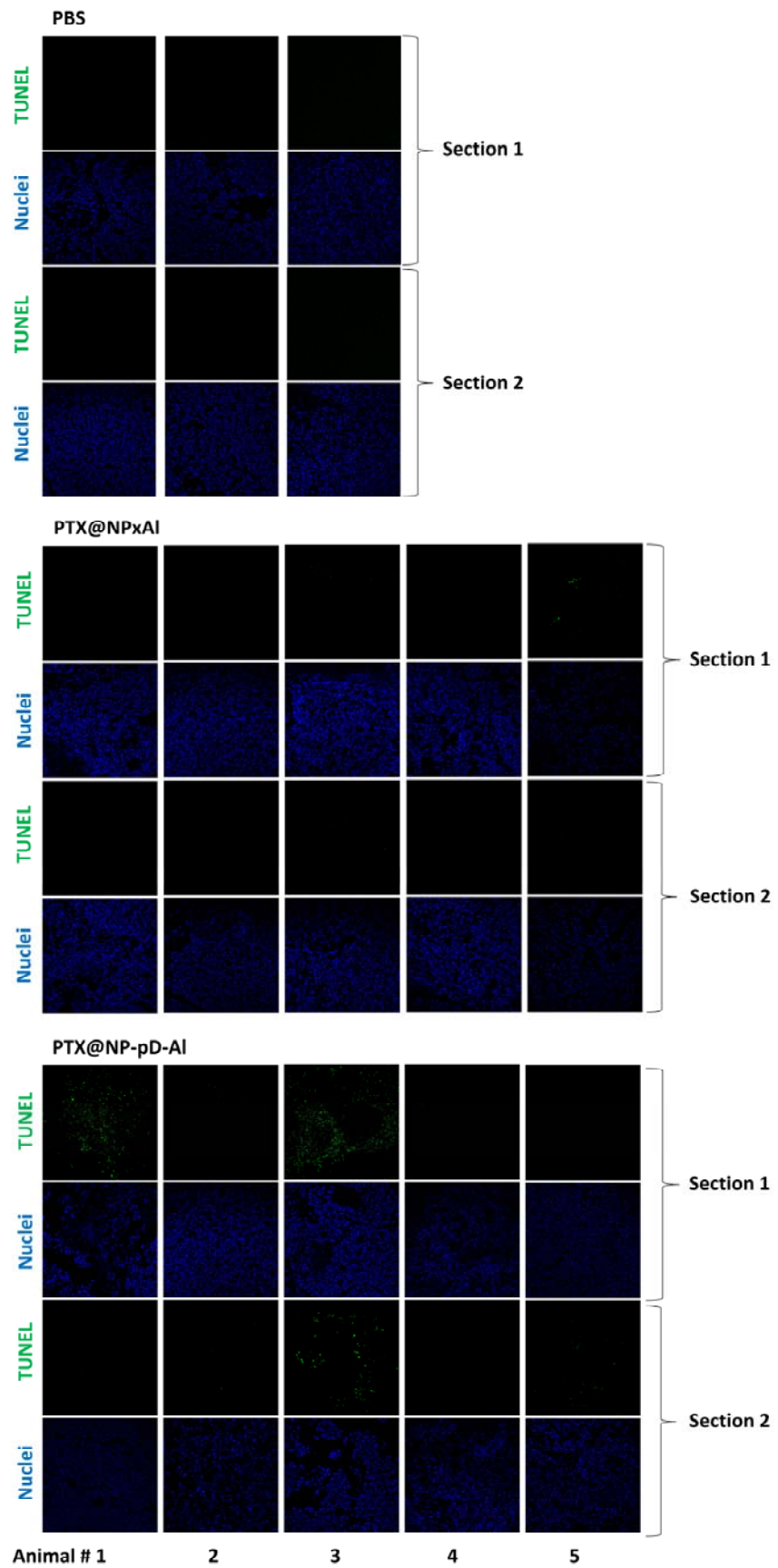


Fig. S15. All images of TUNEL-stained B16F10 tumor sections. Two randomly selected fields were imaged for each animal. Mice were treated with PBS ($n = 3$), PTX@NPxAl ($n = 5$), or PTX@NP-pD-Al ($n = 5$) at a dose equivalent to PTX 15 mg/kg q3d \times 2. One day after the second dose, mice were sacrificed for the analysis. Scale bars = 50 μ m.

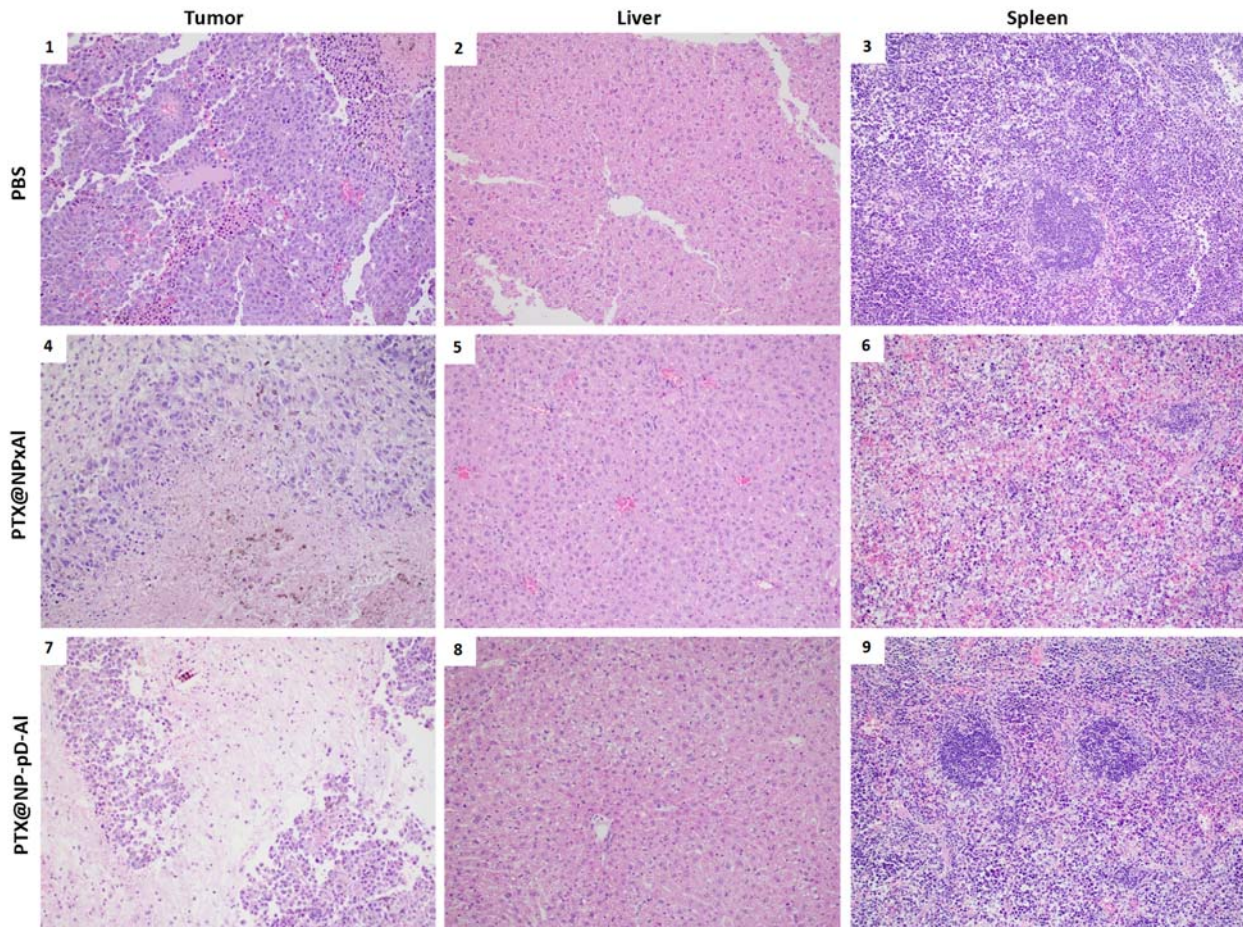


Fig. S16. Photomicrographs (20 \times objective) of PBS treated (1-3) animals with rare tumor hemorrhage, rare vacuolar change within the liver, and normal spleen pathology. PTX@NPxAl treated animals (4-6) demonstrating multifocal tumor necrosis, multifocal vacuolar change within the liver, and lymphoid depletion within the spleen. PTX@NP-pD-Al treated animals (7-9) demonstrating marked tumor necrosis, multifocal vacuolar change within the liver, and lymphoid depletion within the spleen.